International Conference on Space Optics—ICSO 2014

La Caleta, Tenerife, Canary Islands

7–10 October 2014

Edited by Zoran Sodnik, Bruno Cugny, and Nikos Karafolas

PHARAO flight model: optical on ground performance tests

T. Lévèque

B. Faure

F. X. Esnault

O. Grosjean

et al.

esa icso proceedings cnes

International Conference on Space Optics — ICSO 2014, edited by Zoran Sodnik, Nikos Karafolas, Bruno Cugny, Proc. of SPIE Vol. 10563, 105632H · © 2014 ESA and CNES
CCC code: 0277-786X/17/$18 · doi: 10.1117/12.2304277

PHARAO FLIGHT MODEL: OPTICAL "ON GROUND" PERFORMANCE TESTS

T. Lévèque[(1)], B. Faure[(1)], F. X. Esnault[(1)], O. Grosjean[(1)], C. Delaroche[(1)], D. Massonnet[(1)], C. Escande[(1)], Ph. Gasc[(1)], A. Ratsimandresey[(1)], S. Béraud[(1)], F. Buffe[(1)], P. Torresi[(1)], Ph. Larivière[(1)], V. Bernard[(1)], T. Bomer[(2)], S. Thomin[(2)], C. Salomon[(3)], M. Abgrall[(4)], D. Rovera[(4)], I. Moric[(4)], Ph. Laurent[(4)].
[1]*Centre National d'Etudes Spatiales, Toulouse, France.*
[2]*SODERN, Limeil-Brévannes, France.*
[3]*Laboratoire Kastler-Brossel, CNRS, Paris, France.*
[4]*LNE-SYRTE – Observatoire de Paris, Paris, France.*
Email: thomas.leveque@cnes.fr

INTRODUCTION

PHARAO (Projet d'Horloge Atomique par Refroidissement d'Atomes en Orbite), which has been developed by CNES, is the first primary frequency standard specially designed for operation in space. PHARAO is the main instrument of the ESA mission ACES (Atomic Clock Ensemble in Space). ACES payload will be installed on-board the International Space Station (ISS) to perform fundamental physics experiments. All the sub-systems of the Flight Model (FM) have now passed the qualification process and the whole FM of the cold cesium clock, PHARAO, is being assembled and will undergo extensive tests. The expected performances in space are frequency accuracy less than 3.10^{-16} (with a final goal at 10^{-16}) and frequency stability of $10^{-13}\ \tau^{-1/2}$. In this paper, we focus on the laser source performances and the main results on the cold atom manipulation.

I. THE PHARAO/ACES MISSION

A. The ACES Mission

ACES [1] is an ESA mission in fundamental physics which is based on time and frequency comparisons between high performances space clocks and ground based clocks. The space segment will operate a new type of atomic clocks in microgravity environment. The payload (Fig. 1.) will be installed on the NASA developed External Payload Facility pallet of the Columbus laboratory (CEPF) on-board the ISS. The station is orbiting at a mean elevation of 400 km with about a 90 min rotation period and an inclination angle of 51.6 degrees. The number of ISS passes over a European ground station is 5 per day.

Fig. 1. PHARAO flight model before and after integration of the MLI protection.

The clock signal is obtained from the combination of two atomic clocks: a cold cesium clock PHARAO as a primary frequency standard [2] and an active hydrogen maser as a freewheel oscillator. The comparison with earth based clocks is performed by two way time transfer links operating in the microwave domain (MWL) and in the optical domain (ELT). Ground terminals will mainly be located in time and frequency laboratories, while the mission will be operated from the ACES User Support and Operation Center (USOC), installed at CADMOS (Centre d'Aide au Développement de la Microgravite et aux Operations Spatiales) in France. The launch is scheduled on 2016. Planned duration of the mission is 36 months. First 6 months are reserved for functionality verification of instruments and performances evaluation. The first objectives are to study the performances of this first cold atom space clock and reach frequency accuracy lower than 3 x10^{-16} (with a final goal at 10^{-16}) and deliver a timescale with 25 ps/day stability. The microwave link will have to demonstrate the capability to perform phase comparisons between space and ground clocks with a resolution at the level of 0.3 ps over one ISS pass (300 s), 7 ps over 1 day, and 23 ps over 10 days.

B. The cold atom PHARAO space clock

A complete description of the setup and its operation is given in [2]. The PHARAO clock includes 4 sub-systems: the laser source provides laser beams at 852 nm to the cesium tube to manipulate the atoms. The microwave source provides two 9.2 GHz signals to the cesium tube and a 100 MHz signal to the ACES payload. An on-board computer manages the clock operation, sends data and receives telecommand from the ground segment. Since last year, all the subsystems have been qualified and passed the environmental tests, consisting in 3 axis vibrations (~10 g_{rms}) and thermal cycling (-40°C/+60°C). In early 2014, the different PHARAO subsystems have been assembled on the ACES baseplate and wired together. The whole PHARAO instrument has been wrapped with 19 pieces of MLI (Multi-Layer Insulation) to protect from outer radiative heating and to homogenize inner temperature.

II. LASER SOURCE PERFORMANCES

A. Laser source design

The main laser source design challenges arise from the ACES payload accommodation constraints, which impose a high level of compactness, low electric power consumption, a wide range of operating temperature, as well as the need to be operated in both air and vacuum conditions with a sufficient level of performance for testing both PHARAO and ACES.

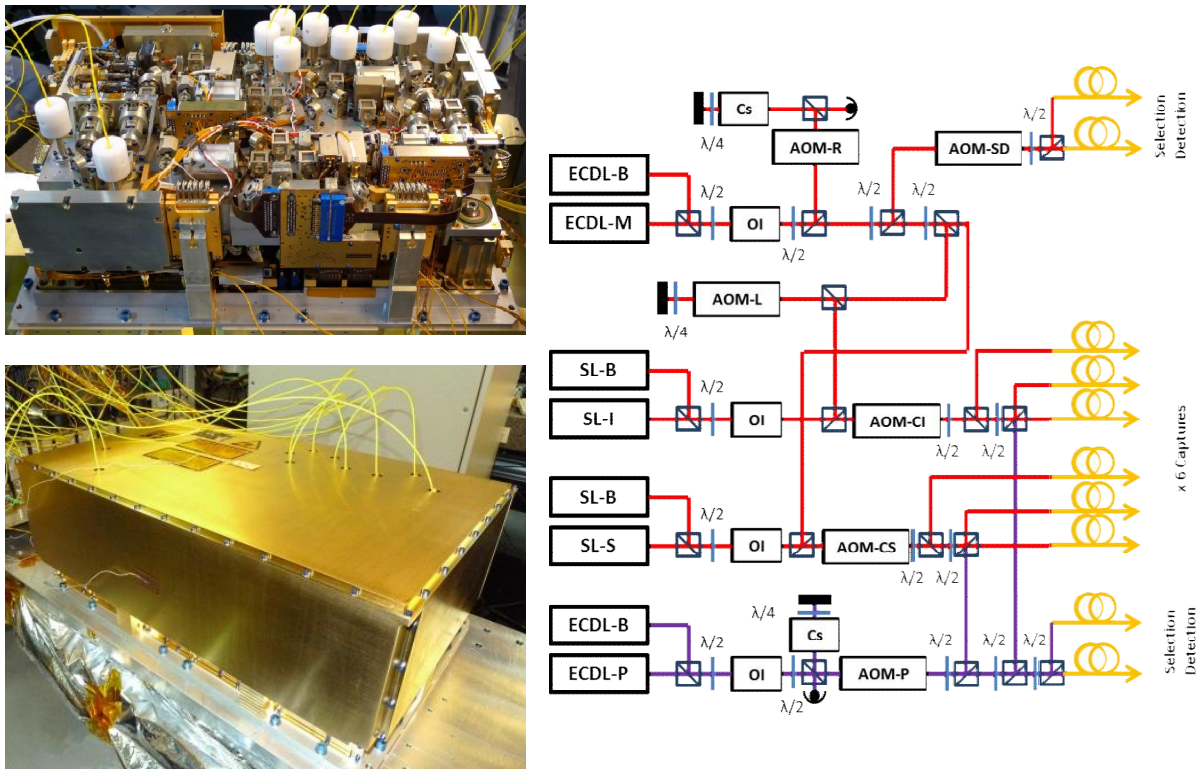

Fig. 2. PHARAO laser source. *Left*: Photograph of the integrated laser source with (*down*) and without (*up*) cover. *Right*: Optical architecture of the laser source. The 8 PZT mobile mirrors and the 5 mechanical shutters are not represented.

The laser source architecture [3] designed by SODERN is shown in Fig. 2. An extended cavity diode laser (ECDL-M) at 852 nm is locked to the saturated absorption crossover resonance of cesium ($|6S_{1/2}$, F=4>→$|6P_{3/2}$, F=4/F=5>) through an acousto-optic modulator (AOM-R). The ECDL design has an intra-cavity etalon for rugged and reliable behavior and reaches a spectral purity 10 to 100 times higher than simple laser diodes [4]. The output power of the ECDL is of 35 mW. To perform the frequency locking, the diode laser current is modulated at 500 kHz and the absorption signal is synchronously demodulated to provide the error signal. This signal is integrated and applied to the diode laser current and to the PZT transducer that drives the cavity length of the ECDL-M. By changing the AOM-R rf frequency the laser frequency can be tuned between 136 and 206

MHz with a rate of 260 kHz/µs. This ECDL/AOM combination provides the frequency reference for all the atom processes: capture, cooling, selection, and detection.

The beam is then split into three beams. One beam is coupled into two optical fibers through an acousto-optic modulator (AOM-SD). It is used for the atomic detection (10 mW) and selection (1,5mW). The laser power is adjusted and controlled by the AOM-SD rf power. This AOM-SD operates at a frequency of 75 MHz. The second part of the beam double passes through an acousto-optic modulator (AOM-L) before injecting a slave diode laser SL-I. The AOM-L frequency can be adjusted from 90 MHz to 87 MHz to launch atoms (from 5cm/s to 5m/s) with the moving molasses method. The third beam injection locks a second slave diode laser SL-S. The slave diode lasers remain locked over a 1 mA current variation. After an optical isolator, the slave laser beam passes through a 90 MHz acousto-optic modulator (AOM-CI and AOM-CS) and is divided into three beams. The two slave lasers then provide the six beams to realize the optical molasses geometry. The AOM-CI and AOM-CS rf power determines the capture and cooling intensities. Each beam is reflected by a mirror mounted on PZT transducers (Cedrat). This allows a fine alignment (θ,ϕ,z) of the beam on the fiber core and a power balancing in each of the three molasses beam pairs. The relative difference between the powers of 2 capture laser beams is lower than 1%. The slave diode laser output power is of 100 mW for an input current of 140 mA (the maximum operational current is of 180 mA). The output power of the capture fibers exceeds 12 mW per fiber.

A second ECDL-P is locked to the cesium crossover resonance ($|6S_{1/2}, F=3\rangle \rightarrow |6P_{3/2}, F= 3/F=4\rangle$). The beam passes through a 101 MHz acousto-optic modulator (AOM-P) and is split into four. Two beams are injected into optical fibers to repump the atoms during selection and detection. The two others are superimposed on the slave beams. In addition, five mechanical shutters ensure complete extinction of the beams (120 dB). Two ECDL-B and two SL-B are used as redundant laser sources. Their beams are superimposed onto the firsts by means of polarizing cubes.

The integrated laser source with dimensions 532 mm x 335 mm x 198 mm is shown in Fig. 2. The optical components are mounted on a double-sided optical bench with dimensions of 450 x 284 x 40 mm. The bench is fixed on the electronic package of the laser source through four dampers and its first resonance frequency is above 150 Hz. The temperature regulation of the bench is ensured by a combination of heaters and Peltier coolers to maintain the temperature at 26°C when the baseplate temperature varies from 10 to 33.5°C. The electronics package is fixed to the PHARAO baseplate. It includes all the laser source drivers. The laser beams are guided toward the cesium tube by 10 polarization-maintaining fibers. The laser power measured inside the cesium tube to feed a servo-loop acting on the AOM-CI and AOM-CS. Ten connectors with insertion loss of 1 dB ensure the link with the cesium tube fibers. The total mass of the laser source is of 22 kg and the electrical consumption is, in average, of 30 W.

B. Frequency noise and RIN measurements

The frequency noise and the residual intensity noise (RIN) of the ECDL-M have been measured at the output of the detection fiber. The envelope of each power spectral density (PSD) is given in Fig. 3. These two features are critical for the performances of the detection system of the atomic clock. In this part, we present an estimation of the impact of the ECDL-M frequency noise and RIN on the PHARAO clock stability.

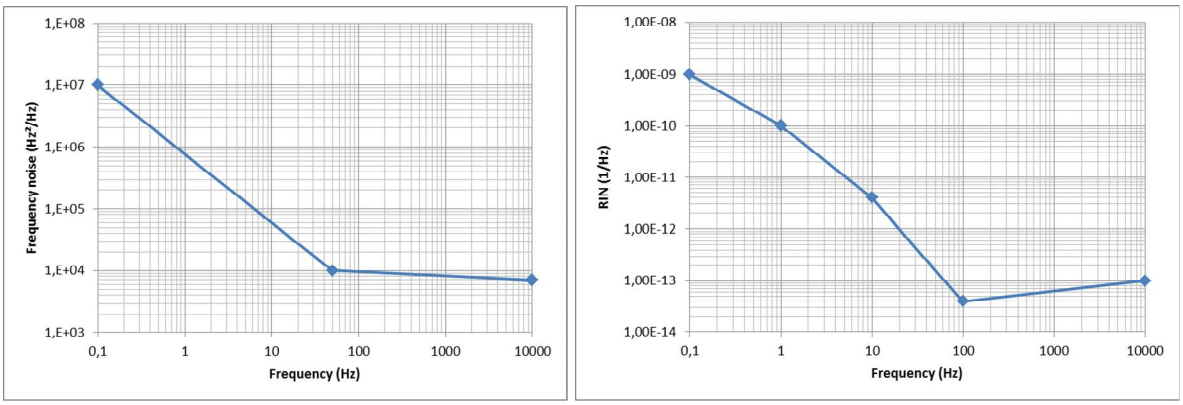

Fig. 3. *Left*: Envelope of the power spectral density of frequency noise. *Right*: Envelope of the power spectral density of relative intensity noise.

The transition probability P of the atoms at the output of the clock is determined by measuring the ratio between the number of atoms in each ground state by a fluorescence method. The atomic cloud passes through two thin detection beams. The fluorescence signals emitted by spontaneous emission are collected on two photodiodes. The areas of these two time-of-flight signals, $A_{|e\rangle}$ and $A_{|f\rangle}$, are proportional to the number of atoms in each ground state.

The relative frequency and intensity fluctuations of the ECDL-M induce variations on the spontaneous emission rate during the detection process. This effect results in a perturbation on the measurement of the atom number present in the detection beams. We denote by $f(t)$ the ratio between the number of atoms present in the first detection beam at a time t and the corresponding total time-of-flight area $A_{|e\rangle}$. At the time $t + \Delta t$, the atoms pass through the second detection beam, leading to fluctuations in the area of flight time $A_{|f\rangle}$. We consider a Gaussian type profile for the time-of-flight signal:

$$f(t) = \frac{1}{\sqrt{2\pi}w}\exp\left(-\frac{t^2}{2w^2}\right) \tag{1}$$

The temporal width of the time-of-flight w is connected to the initial width of the atomic cloud (w_x = 5,52 x 10^{-3} m), the launch speed (v_0) and the width of the velocity distribution of the atomic cloud (w_v = 8 x 10^{-3} m/s). The time-of-flight signal is the result of the convolution between the initial width of the cloud and the width of the velocity distribution weighted by the total flight time t_{tof} of the atoms between the capture and the detection. The temporal width of the flight time is therefore given by:

$$w = \frac{1}{v_0}\sqrt{{w_x}^2 + \left(w_v t_{tof}\right)^2} \tag{2}$$

We therefore neglect the width of the probe compared to the size of the atom cloud at the time of the detection. This assumption is particularly valid when the launching velocity is low. The total flight time t_{tof} is connected to the launching velocity v_0 and the length between the capture zone and the detection zone (L=0.54m). We therefore have $t_{tof} = L/v_0$.

- *Fluctuation of the time-of-flight area:*

The fluctuation of the time of flight area for each ground state |f> and |e> is given by:

$$\delta A_{|f\rangle,|e\rangle} = A_{|f\rangle,|e\rangle} \times \int_{-\infty}^{+\infty} \delta\gamma(t)\, f(t)\, dt \tag{3}$$

Where $\delta\gamma(t)$ is the fluctuation of the spontaneous emission rate.

- *Fluctuation of the transition probability:*

The transition probability P is measured by:

$$P = \frac{A_{|e\rangle}}{A_{|e\rangle} + A_{|f\rangle}} \tag{4}$$

This probability is then affected by a fluctuation δP which can be expressed, in the particular case of mid-fringe measurement, as:

$$\delta P = \frac{1}{2} \times \frac{\delta A_{|e\rangle} - \delta A_{|f\rangle}}{A_{|e\rangle} + A_{|f\rangle}} = \frac{1}{4}\int_{-\infty}^{+\infty} \delta\gamma(t)\left[f(t) - f(t-\Delta t)\right]dt \tag{5}$$

The standard deviation of these fluctuations is then given by:

$${\sigma_{\delta P}}^2 = \int_0^{+\infty} S\_\delta\gamma(f) \cdot \left|H\_\det(f)\right|^2 df \tag{6}$$

Where $S\_\delta\gamma(f)$ is the PSD of the fluctuations of the spontaneous emission and $H\_det(f)$ is the transfer function of the detection system:

$$H\_\det(f) = \frac{1}{4}\left(1 - e^{-2i\pi f\,\Delta t}\right) \times e^{-2\pi^2 f^2 w^2} \tag{7}$$

The PSD of the spontaneous emission rate fluctuations $S\_\delta\gamma(f)$ can be related to the frequency fluctuations ($S\_\upsilon\_LCE(f)$) and to the relative intensity noise (RIN) of the ECDL. In this calculation, we consider the case of unsaturated atoms and of a $\Gamma/2$ red detuned detection laser, thereby maximizing the sensitivity to the laser frequency fluctuations. It is given, at the first order by:

$$S\_\delta\gamma(f) = \left(\frac{4\pi\upsilon_{laser}}{\Gamma}\right)^2 \times S\_\nu\_LCE(f) + S\_RIN(f) \quad (8)$$

The final contribution of the laser noise to the stability of the clock (σ_y) is given by:

$$\sigma_y(\tau) = \frac{2}{\pi Q_{at}} \times \sigma_{\delta P} \times \sqrt{\frac{T_c}{\tau}} \quad (9)$$

Where τ is the integration time, T_c is the cycling time of the clock and Q_{at} is the atomic quality factor. We carry out the numerical application of this calculation for 7 launching velocities v_0. We calculate in each case the contribution of the frequency noise and RIN on the stability of the clock at 1s. The results are summarized in the Tab. 1:

v_0(m/s)	σ_f @ 1s	σ_{RIN} @ 1s
0,15	3,70 x 10^{-16}	1,06 x 10^{-17}
0,20	7,38 x 10^{-16}	2,09 x 10^{-17}
0,30	1,92 x 10^{-15}	5,08 x 10^{-17}
0,60	8,58 x 10^{-15}	1,92 x 10^{-16}
1,00	1,92 x 10^{-14}	3,83 x 10^{-16}
3,00	6,37 x 10^{-14}	1,08 x 10^{-15}
3,54	7,64 x 10^{-14}	1,26 x 10^{-15}

Tab. 1. Expected contribution of the relative frequency noise (σ_f) and RIN (σ_{RIN}) on the stability of the clock at 1s for 7 given launching velocities v_0.

Frequency and intensity noises of the detection lasers have a very small impact on the clock stability, especially for low launching velocities. For high launching velocities, the clock stability is impacted at a non-limiting level compared to quantum projection noise (> 10^{-13} $\tau^{-1/2}$). Thus, the performances of the instrument are not limited by the frequency and intensity noises of detection laser. Moreover, in the calculation, the contribution of laser frequency noise to the clock stability is largely overestimated (Γ/2 detuning). In the real case this contribution is then negligible.

C. Qualification process

The laser source is one of the most critical parts of a cold atom apparatus. It must keep its performances in terms of delivered optical power, linewidth, frequency stability and spectral agility in a space environment. This system must be reliable enough to undergo high level of vibration and must remain operational over a large range of temperature. The validation of the design has been realized through the development of a Structural and Thermal Model (STM) and an Engineering Model (EM). The STM was used to perform the qualification tests and the EM was used to validate the functional performances of the laser source.

In a first time, qualification models representative of each key part of the flight model, where built to study the impact of environmental conditions on their performances. Thus, each component and subsystem of the laser source was submitted to a set of harsh qualification tests. In non-operational conditions, these tests have proven a compatibility of the design with thermal variations (-40°C /+ 60°C) and random vibrations (up to 10,9 g_{RMS}).

Then, the complete FM of the laser source was submitted to a set of acceptance tests. Random vibrations were carried out at a level of 6.5 g_{RMS}. Thermal variations in non-operational conditions were realized between -40°C and +60°C. Optical performances of the flight model, including output power level and laser spectral purity verifications, were performed after each acceptance tests. Finally, the performances of the flight model were tested in operational conditions in the thermal range of +10°C/+33.5°C, corresponding to the actual environmental conditions on-board the ISS. Moreover, Electro-Magnetic Compatibility (EMC) tests were carried out on the EM for qualification and on the FM for acceptance. The laser source functions and the laser beam noise levels (frequency and power) have been verified under vacuum conditions.

III. EARLY RESULTS OF THE PHARAO FLIGHT MODEL

A. Test setup

In early 2014, the different PHARAO subsystems have been assembled on the ACES baseplate and wired together. To mimic in-orbit environment, PHARAO is tested in a vacuum chamber (~2 10^{-6} mbar). This

dramatically changes the thermal behavior of the different sub-systems. Coils surround the chamber to compensate for the earth magnetic field and allow reproducing magnetic orbital variations along the PHARAO main axis.

B. Cold atom manipulation

The first step of the testing phase was to tune all the laser source and cesium tube parameters regarding the capture, the cooling, launching, selection, slicing and detection of the atoms. These set of parameters have been optimized for "on-ground" operation in which the atoms are launched upwards at 3.54 m/s. Some of these parameters will need readjustment once in orbit (e.g. launching velocity can changed at will from 0.05 to 5 m/s) owing to the peculiar behavior of the cold atom cloud in micro-gravity.

- *Cold atom preparation:*

The cold atom preparation is divided in four phases represented of the Fig.4: The capture, the launching, the cooling and the adiabatic cutoff corresponding to different configurations of the beam intensity and detuning.

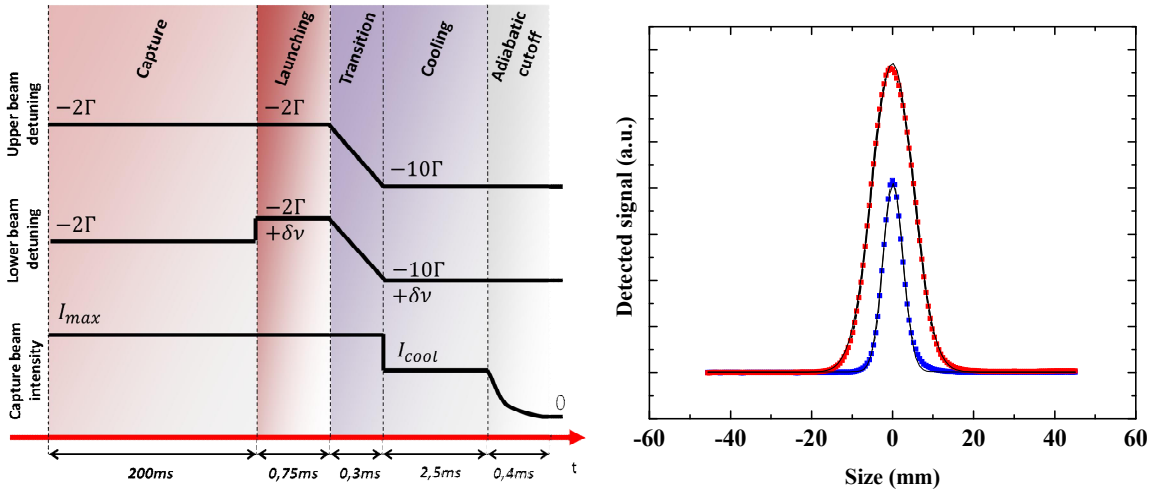

Fig. 4. *Left:* Typical sequence of atom preparation. *Right:* Detected signal, time-of-flight of the atoms. The atomic distribution at the detection is represented without (red points) and with slicing (blue points). Black lines are the Gaussian fits.

During the capture, cesium atoms are loaded from a thermal vapor into an optical molasses. The detuning of the capture beams is set around *-2Γ*. The number of atoms loaded in the molasses can be adjusted by changing the intensity of the capture beams via the AOM-CI and AOM-CS rf power. This signal is measured via a photodiode by a fluorescence method. The atoms are then launched with the moving molasses technique. In this purpose, a frequency shift between the upper and the lower cooling beams is applied through the AOM-L controlling the lower cooling beams detuning. In addition, the atoms are cooled down to a temperature of about 1.2 µK in the molasses by chirping the mean frequency down to *-10Γ* with respect to the cooling transition. During this phase, the intensity of the beams is significantly reduced. The finale preparation stage is an adiabatic cutoff which consists in decreasing exponentially the beam intensity to zero.

The duration and the parameters of each phase are then optimized in order to prepare as much atoms as possible at the lowest temperature in the "on ground" configuration. First, we determine the laser frequency which maximizes the number of cold atoms during the capture phase. The laser power is set at maximum (13.5mW/beam). Then, we tune the AOM-R frequency and record the fluorescence signal. The maximum atom number is obtained when the AOM-R is tuned at 205 MHz, corresponding to the typical value, *-2Γ*, of the laser detuning when an optical molasses technique is used. As the number of detected atoms is large and can saturate the detected signal, the loading time is set to 200 ms and the capture laser power is decreased to 5mW for the "on ground" configuration. The number of atoms is determined from the fluorescence value. With the current set of parameters we can capture up to $4x10^8$ atoms.

Second, the launching and the cooling durations are scanned from 0.4 to 2 ms, the cooling laser power is scanned from 0.5 to 7mW and the cooling frequency detuning from -30 MHz to -80 MHz. The time-of-flight

signal is then recorded for each quadruplet of parameters. All the recorded signals are analyzed to determine the optimal configuration which produces the largest number of detected atoms (ie time-of-flight signal area) and a Gaussian time-of-flight profile. We have retained the following sets of parameters:

- Launching duration: 0.75 ms or 2 ms.
- Cooling duration: 2.5 ms or 1 ms.
- Laser power during cooling phase: 1.69 mW/beam.
- Laser detuning during cooling phase: -45 MHz or -69.8 MHz.

The corresponding detected signal is shown on the Fig. 4. The size of the detected cloud, 16mm, is much larger than the capture laser beams (10.5 mm). During the launch/cooling duration (3ms), the cloud spreads over a distance of 10mm. In microgravity the launch velocity will be about 10 times lower and the spreading effect will be negligible.

- *Cold atom selection:*

Following the launching stage, the atoms are distributed among all Zeeman sublevels of the $|6S_{1/2}, F=4\rangle$ state. Atoms are then selected in the sublevel $m_F=0$. For this purpose, a static magnetic field is applied to lift the degeneracy of the Zeeman sublevels. Atoms in $|6S_{1/2}, F=4, m_F=0\rangle$ are transferred to $|6S_{1/2}, F=3, m_F=0\rangle$ when passing through a microwave cavity. The selected cloud in $|6S_{1/2}, F=3, m_F=0\rangle$ is then sliced by a specific pump beam in order to limit its size. This optional slicing phase will be particularly useful for flight operation with slow launching velocities. After these two selection interactions, any atoms remaining in $|6S_{1/2}, F=4\rangle$ are removed by a pusher beam.

The first step for optimizing the selection system is to verify the efficiency of the pumping selection beam. In this purpose, we scan the pumping selection beam power and record the detection signal. The pump mechanical shutter is opened during all the selection process. For 0.3 mW of pump power, we reach the minimum of atoms, 1%, corresponding to the residual atoms in F=3 after the cooling phase. The power of the selection pumping beam is sufficient for velocity lower than 3.56 m/s. The second step is to slice the cloud. The pumping beam is on at 228ms, off at 235.4 ms and on again at 237.1 ms. The size of the selection laser beam is 2mm and the atomic velocity is 3.2 m/s. During 1.7 ms the atoms cover a distance of 5.44mm. The slice thickness will be about 4.44 mm. The Fig. 4. shows the cloud distribution without and with slicing.

- *Cold atom detection:*

The transition probability *P* of the atoms at the output of the clock is determined by measuring the ratio between the number of atoms in each ground state by a fluorescence method. The detection system is made of two thin probe beams with a pusher beam and a pumping beam in between. After the Ramsey interrogation, the atoms pass through the first probe beam. The fluorescence light emitted by the cycling transition is collected by an imaging system (5.85% efficiency). The output signal, given by the area of the time-of-flight signal, is proportional to the number of atoms into the F=4 state. These detected atoms are then eliminated by the pusher beam. The remaining cloud, made up of atoms in the F=3 state, is optically pumped to the F=4 state while passing through the pumping beam. These atoms are finally detected with the second probe beam.

The first step for optimizing the detection system is to determine the efficiency of the pushing beam, the pumping beam being off. We scan the laser frequency and the laser power and records the number of detected atoms in F=3 and F=4. A good pushing efficiency is given for a detuning of -2 MHz (198 MHz) and a laser power of 2 mW. At higher power the efficiency is practically independent of the frequency. We consider a power of 4 mW and a frequency of 200 MHz as the current set-points. In the second step, we scan the power of the pumping laser. The evolution of the F=3 and F=4 signals are recorded. The measurement shows that, from a pump power of 10 µW, the F=3 signal saturates and the detected signal in F=4 begins to increase. A pump power of 20 µW is then optimum when the atoms velocity is 1.3 m/s in the detection beams. For higher velocities the power margin is sufficient. In standard operation, due to magnetic level selection, and clipping by the microwave cavity apertures we detect typically 1.2×10^6 atoms. This number stays remarkably stable at the 0.5% level over a day.

C. Frequency stability

The Ramsey fringes of the PHARAO clock are shown in Fig.5. Due to deceleration in the gravity field the transit time in each Ramsey interaction zone is 6.7 ms and 10 ms respectively. The free evolution time in

between is 89 ms leading to an "on ground" fringe width of 5.6 Hz. The contrast is reduced to 90% due to the transit times. The good contrast and symmetry of the magnetically sensitive transition m=1 show the very good homogeneity of the magnetic field inside the cesium tube.

We measured the frequency stability against a cryogenic oscillator named ULISS developed by FEMTO-ST laboratory in Besançon, France [5]. When the internal Ultra Stable Oscillator (USO) of the clock is used, the frequency stability is limited by the Dick effect to $3.2 \times 10^{-13}\ \tau^{-1/2}$. This modest performance is expected "on-ground" since the USO characteristics are not optimized for such a short cycle time. When the cryogenic oscillator is used to generate the interrogation signal at 9.192 GHz, the frequency stability is limited by the quantum projection noise to $1.5 \times 10^{-13}\ \tau^{-1/2}$.

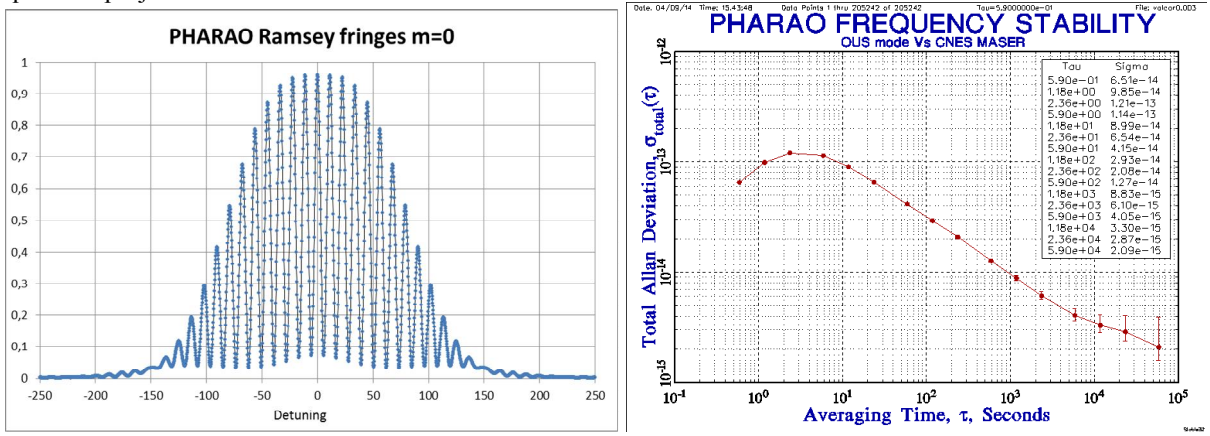

Fig. 5. *Left:* Ramsey fringes on m=0. *Right:* PHARAO frequency stability measured against CNES H-MASER. This measurement lasted about 36 hours.

CONCLUSION

In conclusion, the laser source flight model has been assembled by SODERN. We have demonstrated the compatibility of this model with the PHARAO requirements. Specially, the noise of the laser source has been characterized and its influence on the stability of the clock has been shown to be negligible. The environmental acceptance tests have been carried out successfully. The complete PHARAO flight model has been assembled and extensively tested in CNES. All the aspects of the cold atom manipulation have been characterized and "on ground" trapping and cooling parameters have been determined. The PHARAO flight model has demonstrated a level of stability $3.2 \times 10^{-13}\ \tau^{-1/2}$. Finally, ACES will be assembled in spring of 2015. The launch is envisioned in 2016 by SpaceX.

ACKNOWLEDGMENTS

We would like to thank all the members of the PHARAO industrial team in CNES: Ph. Chatard, C. M. de Graeve, S. Tellier, C. Stepien, L. Fonta, T. Basquin, S. Julien and E. Leynia de la Jarrige for their determinant work in assembling and testing the PHARAO flight model.

REFERENCES

[1] L. Cacciapuoti and C. Salomon, "Space clocks and fundamental tests: The ACES experiment," The European Physical Journal Special Topics, vol. 172, no. 1, pp. 57–68, June 2009.
[2] I. Moric *et al.* "Status of the flight model of the cold atoms space clock PHARAO," Proceedings, 2013 EFTF & IEEE Int. Frequency Control Symp. Joint meeting, Prague, Czech Republic, July 21-25, 2013.
[3] Ph. Laurent *et al.* "Design of the cold atom PHARAO space clock and initial test results", Appl. Phys. B, vol. 84, pp. 683-690, August 2006.
[4] X. Baillard *et al.* "Interference-filterstabilized external-cavity diode lasers", Opt. Commun, vol. 266, pp. 609-613, 2006.
[5] V. Giordano *et al.* "New-Generation of Cryogenic Sapphire Microwave Oscillators for Space, Metrology, and Scientific Applications." Rev. Sci. Instrum. vol. 83, 085113, pp.1-6, August 2012.